Electronic Supplementary Material (ESI) for Physical Chemistry Chemical Physics.

Accelerating supramolecular aggregation by molecular sliding

Wenjing Zhao,[+a] Hongxu Du,[+a] Yijie Xia,[+b] Siyu Xie,[a] Yu-Peng Huang,[b] Tieqi Xu,[c] Jie Zhang,*[a] Yi Qin Gao,* [b] and Xinhua Wan*[a]

[a] W. Zhao, H. Du, S. Xie, Prof. J. Zhang, Prof. X. Wan
Beijing National Laboratory for Molecular Sciences, Key Laboratory of Polymer Chemistry and Physics of Ministry of Education, College of Chemistry and Molecular Engineering, Peking University, Beijing 100871, China.
E-mail:xhwan@pku.edu.cn; jz10@pku.edu.cn

[b] Y. Xia, Y. Huang, Prof. Y. Gao
Beijing National Laboratory for Molecular Sciences, College of Chemistry and Molecular Engineering, Peking University, Beijing 100871, China.
E-mail: gaoyq@pku.edu.cn

[c] Prof. T. Xu
State Key Laboratory of Fine Chemicals, College of Chemistry, Dalian University of Technology, Dalian 116024, China.

[+] These authors contributed equally to this work.

Table of Contents

1. Materials and General Considerations

*i*P2VP (Mn=1.45×10^5, mmmm>99%) was prepared by the coordination polymerization method reported in the literature [S1], *a*P2VP (Mn=1.59×10^5) were purchased from Shanghai Zhenzhun Biotechnology Co., Ltd. (+/-)-Camphorsulfonic acids (CSA, 99%) and 2-methlypyridine (2MPy, 99%) were purchased from J&K Scientific Ltd and used without any further purification. 4-Amino-benzenesulfonic acid monosodium salt (Macklin, 97%), phenol (Aladdin, 99%), sodium nitrite (Mreda, AR), 1-Bromooctane (Sigma-Aldrich, 99%), tetrabutylammonium bromide (Aladdin, 99%), anhydrous potassium carbonate (XiLong Scientific, 99%), hydrochloric acid (XiLong Scientific, AR grade), sodium hydroxide (XiLong Scientific, AR grade) all were used as purchased. Chloroform (Beijing Chemical Co., HPLC grade), ethyl acetate (Concord Technology, AR grade), acetone (Concord Technology, AR grade), N, N-dimethylformamide (Concord Technology, AR grade) and methanol (Concord Technology, AR grade) were directly used without further purification.

^{1}H NMR and nuclear Overhauser effect spectroscopy (NOESY) were recorded on a Bruker AVANCE-III spectrometer (500MHz) in $CDCl_3$ at with tetramethylsilane (TMS) as internal standard. FT-IR spectra were collected on a Bruker Tensor 27 spectrometer at room temperature in $CDCl_3$ in a KBr cell with 0.25 mm thickness. Circular dichroism (CD) and ultraviolet absorption (UV) spectra were recorded simultaneously on a JASCO J-810 spectrometer with a 10 mm quartz cell at ambient temperature. Dynamic light scattering data were recorded with a vertically polarized, 100 mW solid-state laser (GXC-III, CNI, Changchun, China) performing at 633 nm as the light source, and a BI-TurboCo digital correlator (Brookhaven Instruments Corp.) to collect and process data. The fluorescence spectrum of the complex was measured on Edinburgh liquid helium temperature-changing steady-state transient fluorescence/phosphorescence spectrometer (3 K-300 K), FLS980, using a four-sided light-transmitting fluorescent cell with an optical path of 10 mm.

2. Experimental Section

2.1 Synthesis of Azo-SO_3H

1. 4-((4-(octyloxy)phenyl)diazenyl)benzenesulfonic acid

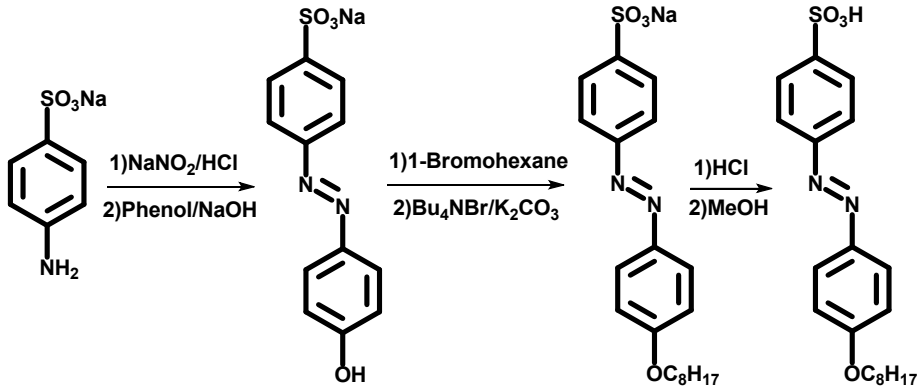

Scheme S1 Synthetic routes of Azo-O_8-SO_3H

The synthetic route is shown in **Scheme S1**. First, 4-Amino-benzenesulfonic acid monosodium salt (3 g, 15.4 mmol) and sodium nitrite (1.17 g, 16.9 mmol) were dissolved in 20 ml deionized water. Then cooled to 0 ℃ using ice bath and added 3.15 ml concentrated hydrochloric acid (38.5 mmol), stirred vigorously for 20min. After that, 10 ml aqueous solution containing NaOH (1.27 g 30.8 mmol) and phenol (1.45 g, 15.4 mmol) was added slowly in above solution, orange precipitate was produced during the dripping. Then the reaction was stirred at 0 ℃ for 3 hours, at room temperature for 1 hour, and finally at 80 ℃ until the solution became clear. Adjusted the pH of the solution to 7 with NaCl. After the reaction was completed, cooled to room temperature, the pH of the solution was adjusted to 7 with NaCl, and the resulting precipitate was washed with chloroform and acetone. Then recrystallized in water, filtered, dried in vacuum at 70 ℃for 24 hours, giving orange-red powder (4.12 g, yield 89%)

Dissolved the above product (0.6 g, 2 mmol) in 50 ml anhydrous DMF, added 1-bromooctane (0.64 g, 3.3 mmol), anhydrous potassium carbonate (0.57 g, 4.1 mmol), and a catalytic amount of tetrabutylammonium bromide. The reaction was stirred at 60 ℃ for 48 h. Then filtered, and washed the precipitate with deionized water and ethyl acetate successively. Vacuum dried at 80 ℃for more than 1 day, giving orange-red powder. The obtained powder was dissolved in a mixed solvent of deionized water/methanol/N,N-dimethylformamide, and excessive concentrated hydrochloric acid was slowly added, stirred overnight. Then extracted with

chloroform, and the solvent was removed by rotary evaporation. Finally vacuum dried at 80 ℃ for more than 1 day, giving orange-red powder.(0.39g, yield 50%).

^{1}H NMR (400 MHz, DMSO-*d*6, δ, ppm): 7.93 – 7.87 (m, 2H), 7.85 – 7.73 (m, 4H), 7.18 – 7.07 (m, 2H), 4.08 (t, *J* = 6.5 Hz, 2H), 1.80 – 1.69 (m, 2H), 1.41 (dt, *J* = 16.1, 8.2 Hz, 2H), 1.35 – 1.22 (m, 8H), 0.87 (t, *J* = 6.8 Hz, 3H). **^{13}C NMR** (151 MHz, DMSO-*d*6, δ, ppm): 161.67 (s), 151.81 (s), 149.98 (s), 146.10 (s), 126.70 (s), 124.71 (s), 121.83 (s), 115.08 (s), 68.05 (s), 39.95 (s), 31.28 (s), 28.84 – 28.51 (m), 25.52 (s), 22.13 (s), 14.00 (s). **ESI-HRMS** (m/z): $[M-H]^-$ Calculated for $C_{20}H_{25}N_2SO_4^+$, 389.1541; Found, 389.1538.

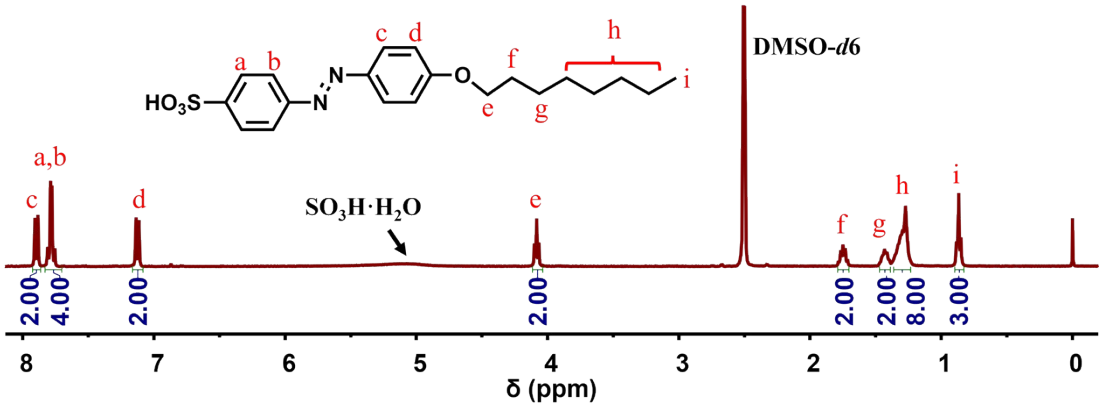

Figure S1 ^{1}H NMR (400 MHz) spectra of Azo-SO_3H in DMSO-*d*6

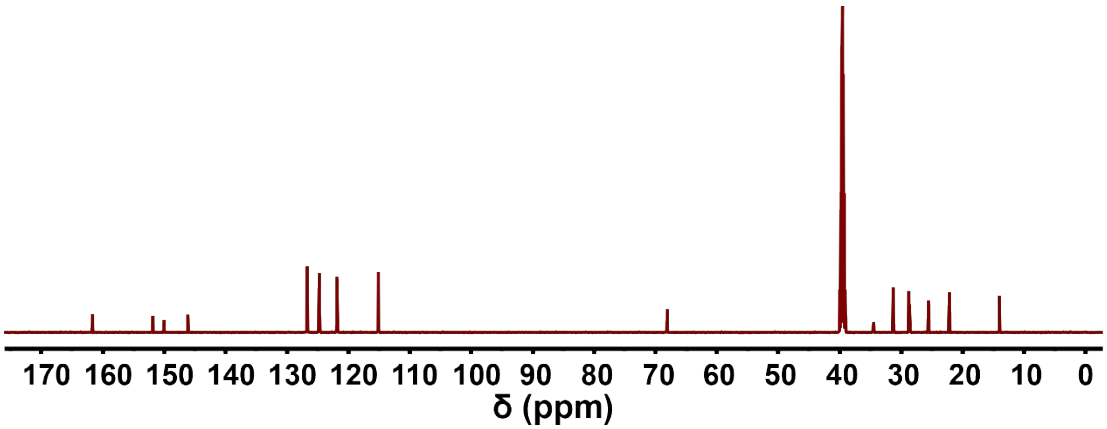

Figure S2 ^{13}C NMR (151 MHz) spectra of Azo-SO_3H in DMSO-*d*6

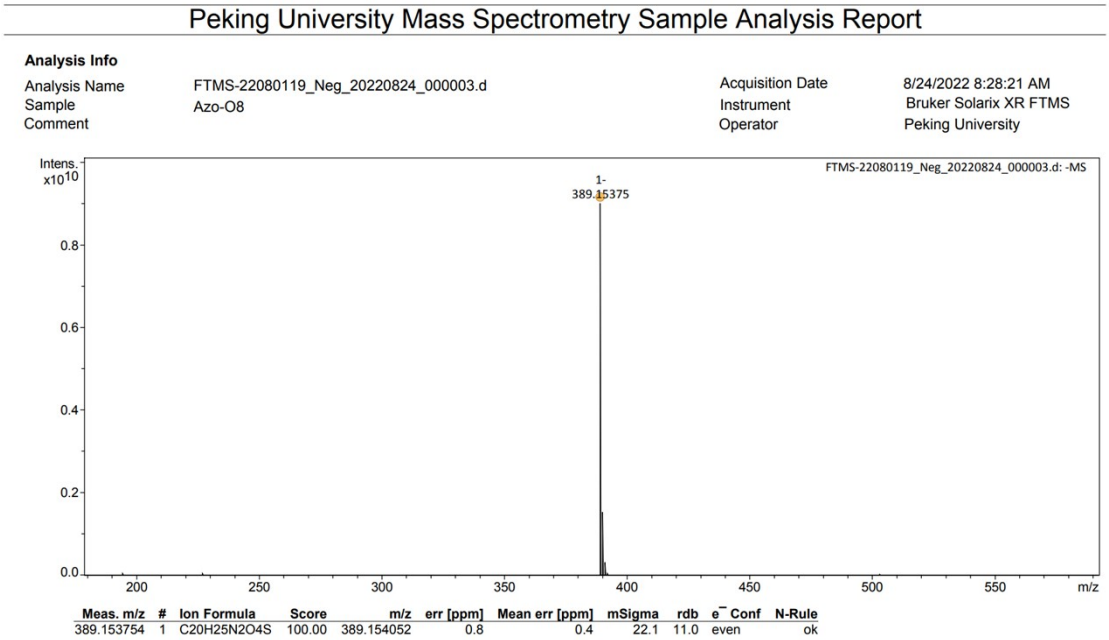

Figure S3 ESI–HRMS spectra of Azo-SO_3H in MeOH.

2.2 Preparation of *i*P2VP/(-)-CSA/Azo-SO_3H complex

Stock solutions of *i*P2VP (6.96 mM), (-)-CSA (5.86 mM), and Azo-SO_3H (0.88 mM) in chloroform were prepared in three separate bottles equipped with screw caps. Into a 10 ml calibrated tubes were introduced sequentially *i*P2VP (144 **μ**L), (-)-CSA (137 **μ**L), and Azo-SO_3H (227 **μ**L) solutions. Afterward chloroform was then added to make the volume up to 10 ml. The final concentration of the complex was 1.0×10^{-4} M, and the molar ratio of *i*P2VP, (-)-CSA, and Azo-SO_3H was 1:0.8:0.2. Other complexes were obtained in a similar method.

2.3 Spectroscopical characterization of acid-based complexes during UV irradiation

The as-prepared acid-based complexes were irradiated by UV light to trigger the photoisomerization and aggregation processes. The LED is purchased from Shanghai Yuntong Electronic Technology Co., Ltd. The LED is a point light source with full width half max of 10±2 nm and the center wavelength located at 365 nm. The UV light irradiated at the sample with a circle light spot, the light intensity at the sample is 30 mW/cm^2. Absorption (JASCO J-810), CD (JASCO J-810) and fluorescence (FLS1000) spectra of complexes were recorded after exposure to UV irradiation for different time intervals.

2.4 Standard procedure for *in-situ* monitoring the absorption intensities at 360 nm

They were measured by using the pump-probe technique. A LED (365 nm) was used as a pumping beam to generate UV light. JASCO J-810 was used to provide a probe beam to detect time-dependent absorption signals at a fixed wavelength (360 nm) when applying UV illuminations to the samples. A cutoff filter (FL 355-10, purchased from Thorlabs) was used to reduce stray light from the pumping laser.

Considering identical concentrations of azo anions in this work, we used relative conversions of monomeric *cis* azo into *cis* aggregates to monitor the aggregation process under different cases. The relative rate accelerations were derived the slope of the absorption of complexes vs. UV irradiation time for the first 10-40% of monomeric *cis* azo anions conversion.

3. Additional Figures

3.1 FT-IR and Nuclear Magnetic Resonance (NMR) Spectra of sulfonic sliders, pyridine pendants footholds and polymeric tracks

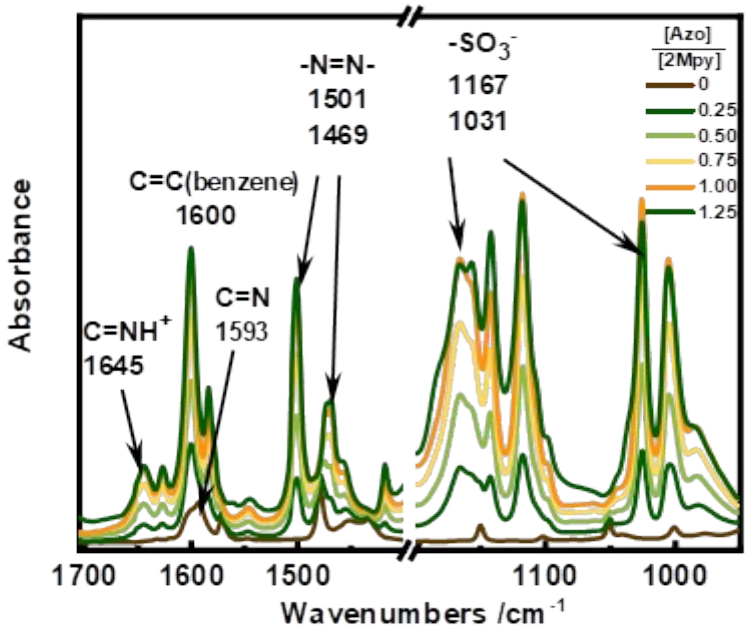

Figure S4 FT-IR spectra of 2MPy-Azo complex with various acid-base ratio in $CDCl_3$. The concentration of 2MPy was *ca.*4 mg/ml.

In Figure S1, with the addition of Azo-SO_3H, the absorption of pyridine C=N at 1593

cm^{-1} of 2MPy decreased proportionally with Azo-SO_3H to 2MPy ratios, a new band at 1645 cm^{-1} due to the $C=N^+$ stretching vibration appeared and increased to the acid-base ratio. In addition, 1167 cm^{-1} and 1032 cm^{-1} are the stretching vibration peak of SO_3^-, 1600 cm^{-1} is the band of benzene, 1501 and 1469 cm^{-1} are characteristic vibration band of -N=N- [S2,S3]. These results demonstrated the formation of ionic bond between 2MPy and Azo-SO_3H.

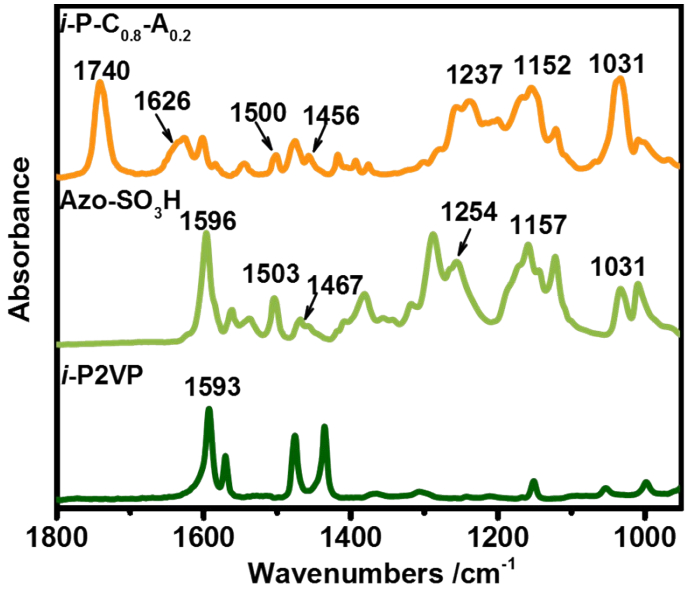

Figure S5 FT-IR spectra of *i*P2VP、Azo-SO_3H and *i*P2VP/(-)-CSA_{80}/Azo-SO_3H_{20} complex with various acid-base ratio in $CDCl_3$. The concentration was *ca.*4 mg/ml.

After mixing the *i*P2VP、Azo-SO_3H with proper molar fraction, typical band shifts were observed in the complex of *i*P2VP/(-)-CSA_{80}/Azo-SO_3H_{20}. As show in Figure S2, 1596 cm^{-1} is the characteristic peak of azobenzene benzene ring, 1503 cm^{-1}, 1467 cm^{-1} is the characteristic peak of -N=N-, 1254 cm^{-1} is the stretching vibration peak of -C-N-. When acid-base complexes were formed, due to the change of the electronic effect of the sulfonic acid group, the characteristic peak of -N=N- shifted from 1503 cm^{-1}, 1467 cm^{-1} to 1500 cm^{-1}, 1456 cm^{-1}, respectively. Also, the characteristic peak of –C-N- shifted form 1254 cm^{-1} to 1237 cm^{-1}, SO_3^{2-} shifted from 1157 cm^{-1} ,1031cm^{-1} to 1152 cm^{-1}, 1031 cm^{-1}, and accompanying with the changes of the relative intensities of characteristic peak.[S3] These results demonstrated the formation of ionic interactions between Azo/CSA sliders and *i*P2VP tracks.

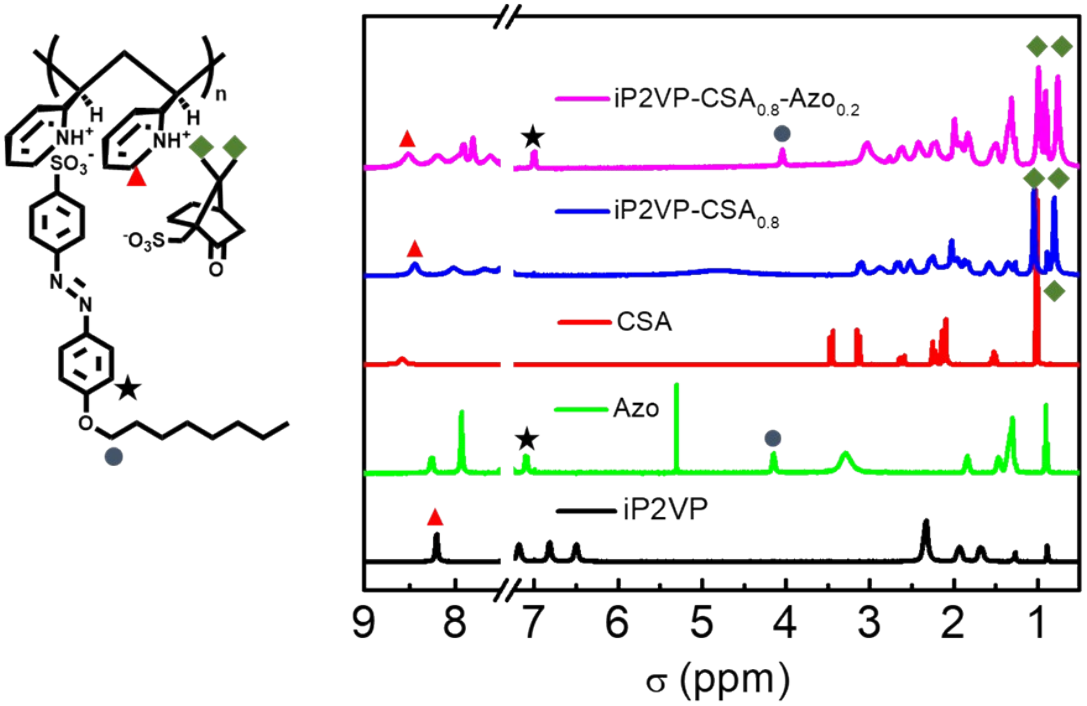

Figure S6 Chemical shifts of the pyridyl proton of *i*P2VP▲, α position of the alkoxy chain●and ortho position of azophenyl ★ of the Azo, methyl protons of (-)-CSA◆ at various complexation ratios. The concentration of *i*P2VP was ca. $1.9*10^{-2}$M.

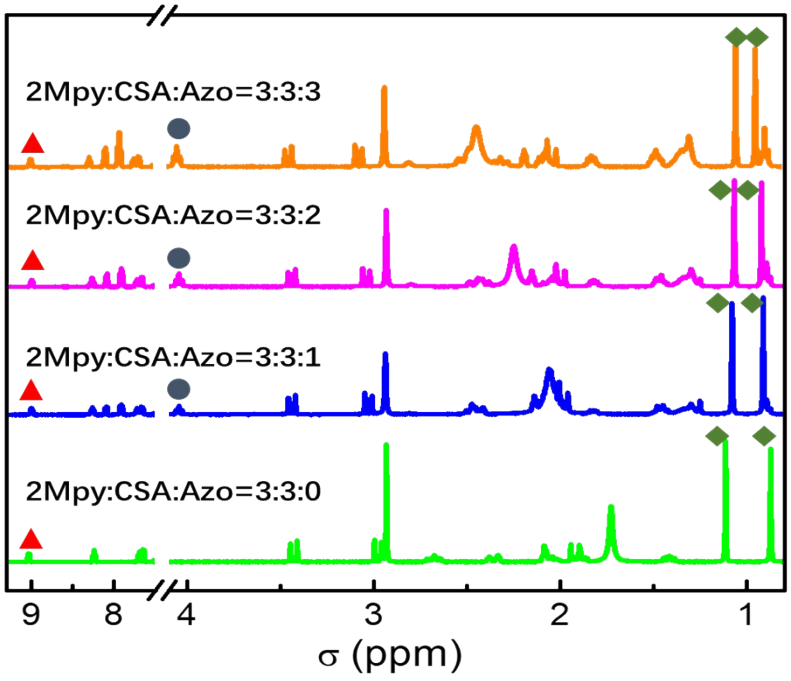

Figure S7 Chemical shifts of the pyridyl proton of 2MPy▲, ortho position of azophenyl ●, methyl protons of (-)-CSA◆ during the titration of 2MPy-(-)-CSA (1.0:1.0, mol:mol) complex with Azo. The concentration of 2MPy was ca. $1.9*10^{-2}$M.

The formation of ionic bond between *i*P2VP and Azo/CSA sliders has also been

proved by ^{1}H NMR titration experiments. The chemical shifts of pyridyl proton of *i*P2VP, α position of the alkoxy chain, ortho position of azophenyl and the methyl protons of (-)-CSA were denoted by ▲,●, ★ and ◆ in Figure S3, respectively. These chemical shift was proportional to the complexation ratio, indicating that the *i*P2VP/(-)-CSA/Azo-SO_3H complexation equilibrium had a very fast exchange rate compared with the NMR time scale. The maximum chemical shift of the methyl group of *i*P2VP was 0.3 ppm, suggesting ionic bond was formed between *i*P2VP and (-)-CSA and Azo-SO_3H.[S4]

Furthermore, during the process of titrating 2MPy/(-)-CSA (1.0:1.0, mol:mol) complex with Azo, the chemical shifts of pyridyl proton, methyl protons of 2MPy remained unchanged, suggesting that 2MPy still existed as protonation form (Figure S4). However, the chemical shifts of methyl protons of (-)-CSA gradually got closer, indicating that the original bound (-)-CSA was substituted by Azo, due to the stronger acidity of the latter species.

3.2 ^{1}H NMR spectra, FT-IR spectra, absorption spectra, fluorescence spectra and Rh of acid-based complex during the UV irradiation

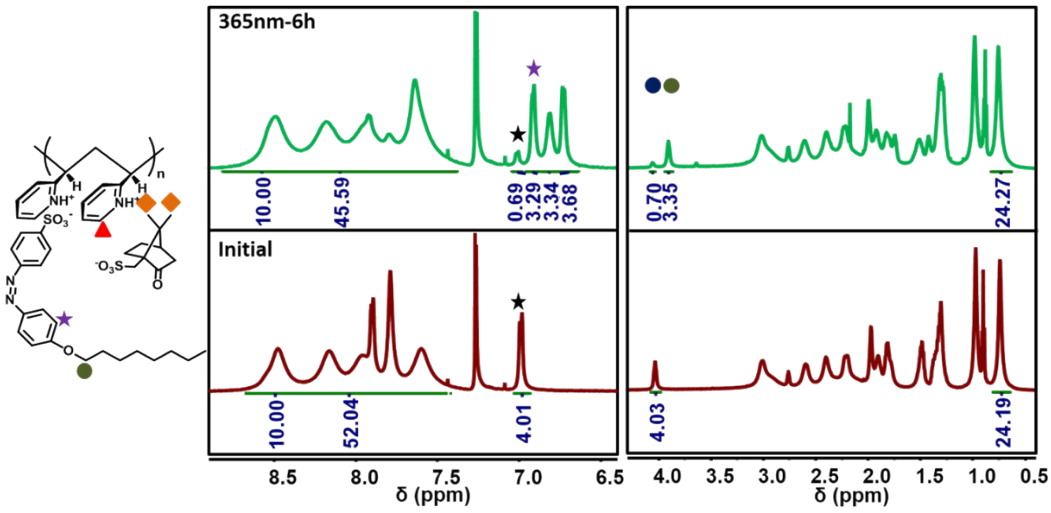

Figure S8 ^{1}H NMR sperctra of *i*P2VP-(-)-$CSA_{0.8}$-$Azo_{0.2}$ before and after photo-isomerization. Chemical shifts of α position of the alkoxy chain●/●and ortho position of azophenyl ★ / ★.The concentration of *i*P2VP was ca. 1.9*10^{-2}M.

As shown in **Figure S5**, before UV irradiation, the H of the azo overlaps with the H

of the pyridine ring in the range of 7.5-8 ppm (except ★), If the number of pyridine units is set to 10, there will be 2 Azo molecules and 8 CSA molecules, So the total number of H in the aromatic ring zone=4*10+(2+4) * 2=52. After UV irradiation, 82.5% of Azo changed from *trans* to *cis* (the number of ★ is 3.3). the integral of ●/●also show that the ratio of *trans-cis* isomerization is about 82.5%.

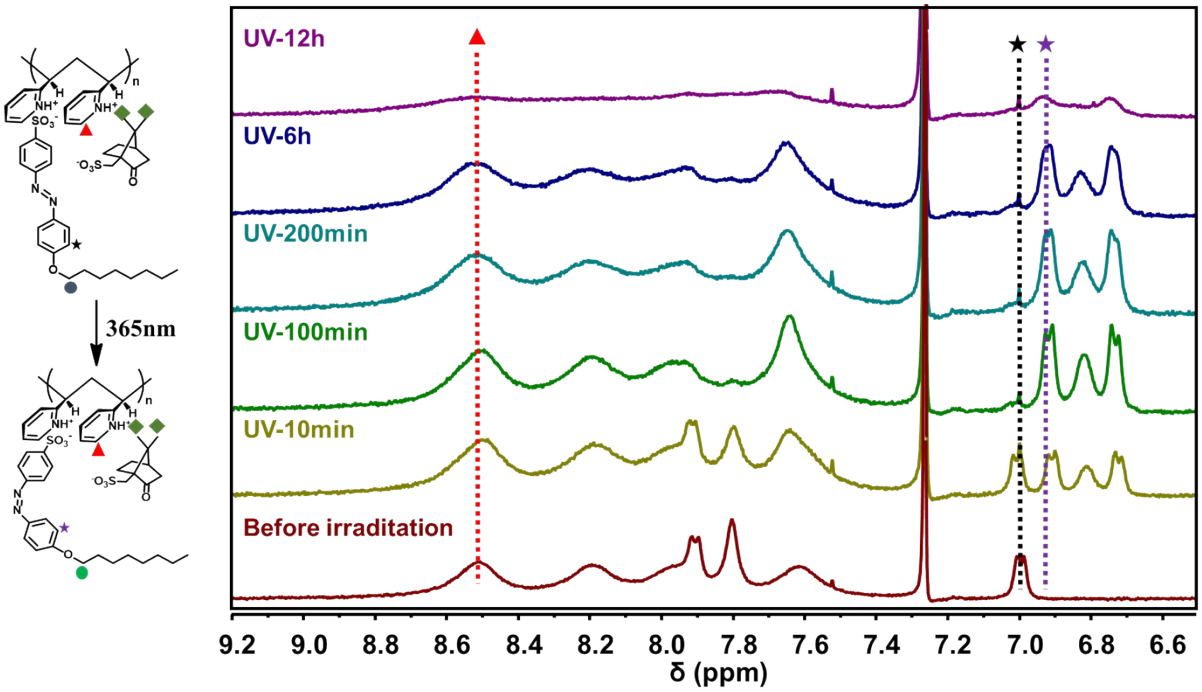

Figure S9 Chemical shifts of the pyridyl proton of *i*P2VP▲, α position of the alkoxy chain● and ortho position of azophenyl ★ of the Azo of *i*P2VP/(-)-CSA_{80}/Azo-SO_3H_{20} before and after UV irradiation with different time. The concentration of *i*P2VP was ca. $1.9*10^{-2}$M.

As shown in **Figure S6**, the ^{1}H NMR spectrum of the *i*P2VP/(-)-CSA_{80}/Azo-SO_3H_{20} under UV irradiation were monitored. It was found that Azo underwent *trans* to *cis* isomerization within 100 min. With prolonging the irradiation time, the chemical shift no longer changes, but it becomes drastically broadened, which indicates that the aggregation of cis-Azo occurs.

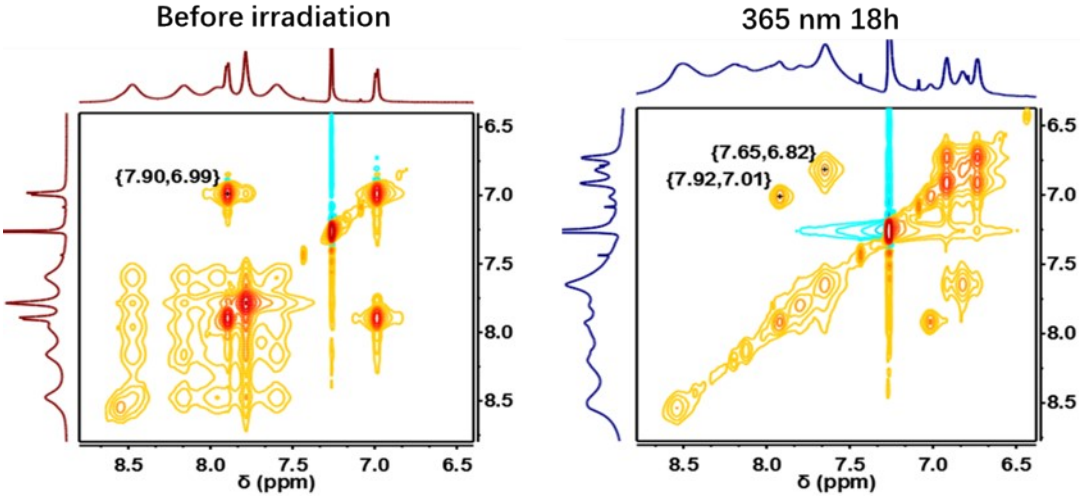

Figure S10 NOESY spectra of *i*P2VP/(-)-CSA_{80}/Azo-SO_3H_{20} before and after UV irradiation for 18 hours in $CDCl_3$. The concentration of *i*P2VP was ca. $1.9*10^{-2}$M.

Figure S10 shows the NOESY spectrum of acid-base complex before and after UV irradiation in $CDCl_3$, the aromatic hydrogens were strongly correlated before UV irradiation, demonstrating the pendant pyridines were relatively close from each other. Nonetheless, after UV irradiation, these pendants got far away to each other, as evidenced by the disappearance of intense cross circles in the NOESY spectrum. Meanwhile, a strong correlation signal attributed to Azo sliders can be observed after UV irradiation, indicating that the Azo sliders got closer to each other.

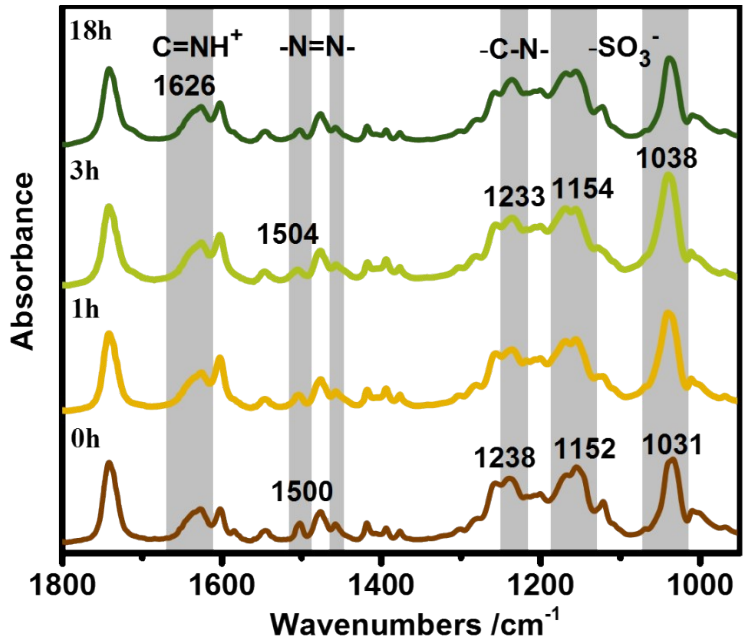

Figure S11 FT-IR spectra of *i*P2VP/(-)-CSA_{80}/Azo-SO_3H_{20} before (brown line) and after UV irradiation with different time in $CDCl_3$. The concentration of *i*P2VP was *ca.*4 mg/ml.

It can be determined by ^{1}H NMR spectra that the photo-isomerization is complete after 3 hours of irradiation. The IR spectra of the solution at different irradiation timeare shown in the Figure S7. After 3 hours of UV irradiation, the characteristic band of -N=N- shifted from 1500 cm^{-1}to 1504 cm^{-1}, because the main azo stretch for *cis*-Azo appears at a higher frequency compared to that for *trans*-Azo due to increased non-planarity, leading to greater double bond character in N=N. The characteristic peak of –C-N- shifts from 1238 cm^{-1} to 1233 cm^{-1} because *trans*-Azo is slightly distorted from planarity whereas *cis*-Azo is completely nonplanar. *Cis*-Azo exhibits more single-bond character for the CN bond, because of which the CN stretch appears at lower wavenumbers for *cis*-Azo relative to that for *trans*-Azo. [4] After further irradiation, no further changes in the characteristic peaks caused by aggregation can be seen from the IR spectrum.

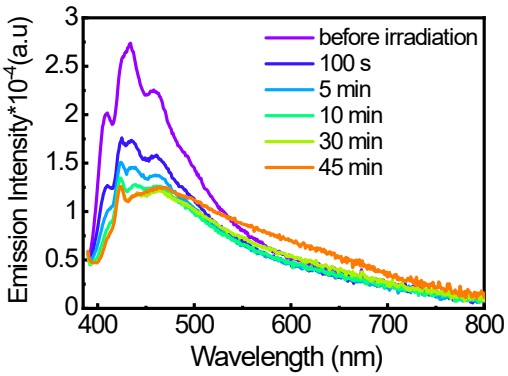

Figure S12 Fluorescence spectra acquired during photoisomerization and aggregation processesof *i*P2VP/Azo-SO_3H_{20} (λ_{ex}=370 nm)

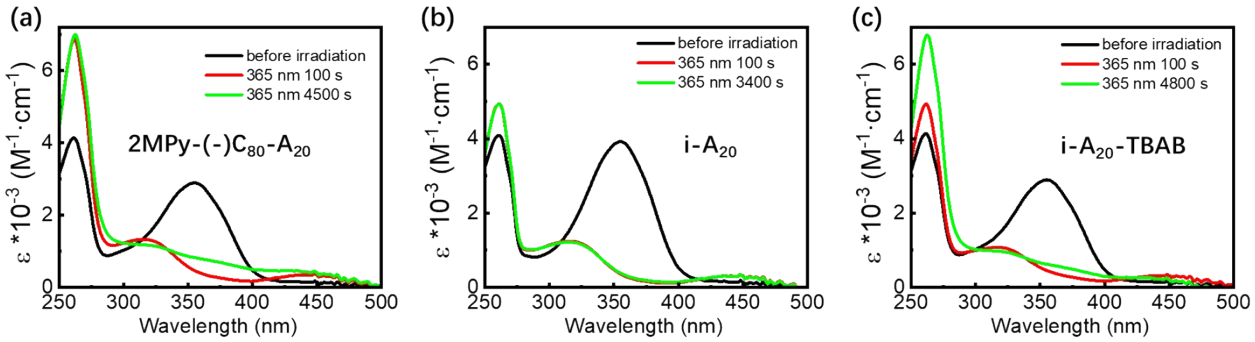

Figure S13 Absorption spectra of 2MPy/(-)-CSA_{80}/Azo-SO_3H_{20}, *i*P2VP/Azo-SO_3H_{20} and *i*P2VP/Azo-SO_3H_{20}-TBAB before and after UV irradiation.

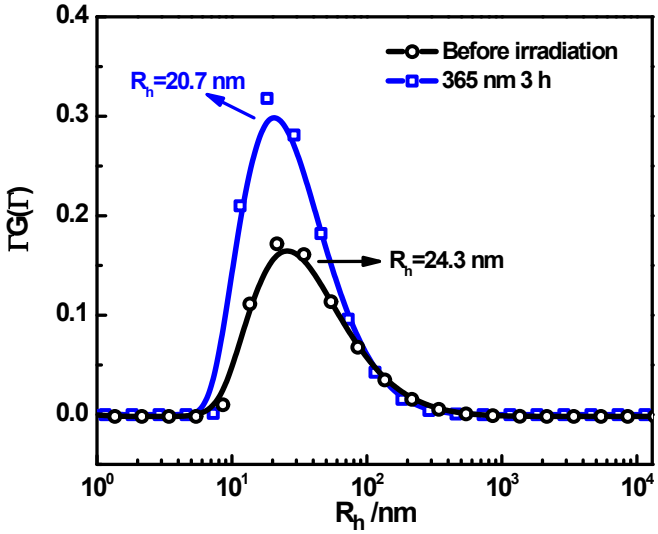

Figure S14 The hydration radius Rh of *i*P2VP/(-)-CSA$_{80}$/Azo-SO$_3$H$_{20}$ before (black line) and after UV irradiation with 3 hours (blue line) in CHCl$_3$. The concentration of *i*P2VP was ca. 0.64 mg/ml.

After being irradiated by UV light, slightly decreased hydration radius（R_h）of complexes (from 23.4 nm to 20.7 nm) were observed (**Fig. S10**). This result suggested that the aggregation of Azo sliders took place on one track but not between adjacent tracks.

3.3 Different aggregate rates of azo sliders based on diffusional dimensions and polymeric tracks

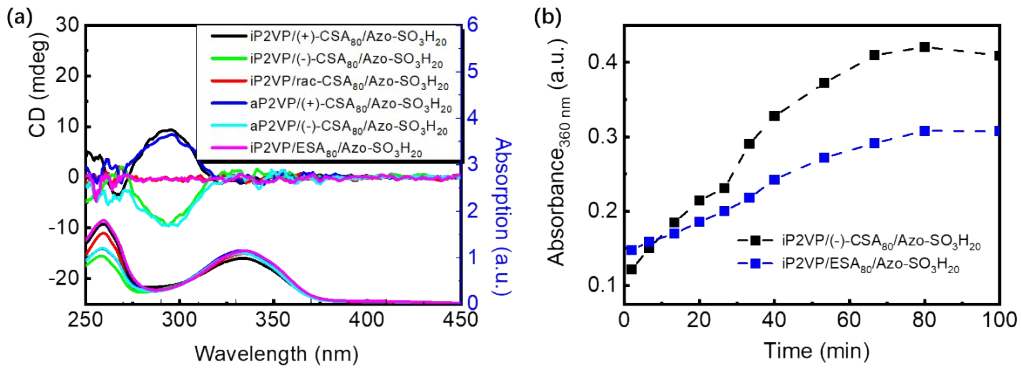

Figure S15 (a) CD and absorption spectra of acid-based complexes with (+)-CSA, (-)-CSA, *rac*-CSA, and ESA as molecular sliders and with *a*P2VP as polymeric tracks. (b) Absorption intensity of azo sliders against UV irradiation time at the wavelength of 360 nm acquired from *i*P2VP/(-)-CSA$_{80}$/Azo-SO$_3$H$_{20}$ and *i*P2VP/ESA$_{80}$/Azo-SO$_3$H$_{20}$, respectively.

Table S1. Relative rate accelerations in the presence of different polymeric tracks or in different diffusional dimensions calculated from three independent measurements.

Complex	Slope*10^{-3}	Rate acceleration
***i*P2VP/(-)-CSA$_{80}$/Azo-SO$_3$H$_{20}$**	1.43±0.839	1
***i*P2VP/(+)-CSA$_{80}$/Azo-SO$_3$H$_{20}$**	1.41±0.687	1.01
***i*P2VP/(-)-CSA$_{80}$/Azo-SO$_3$H$_{20}$/TBAB**	4.91±2.557	0.29
***a*P2VP/(-)-CSA$_{80}$/Azo-SO$_3$H$_{20}$**	0.26±0.191	5.42
***i*P2VP/*rac*-CSA$_{80}$/Azo-SO$_3$H$_{20}$**	0.14±0.07	10.19
2MPy/(-)-CSA$_{20}$/Azo-SO$_3$H$_{20}$	0.056±0.015	25.46
***i*P2VP/Azo-SO$_3$H$_{20}$**	0.01	142
***i*P2VP/Azo-SO$_3$H$_{20}$/TBAB**	1.21±0.014	1.18

4. Molecular Dynamic Simulations

4.1 Systems and methods

Atomistic molecular dynamics (MD) simulations were carried out to clarify the diffusion on polymeric tracks. A 100-monomer *i*P2VP track was selected to represent a polymeric tracks. The following cases were simulated: (a) *i*P2VP/(-)-CSA$_{80}$/Azo-SO$_3$H$_{20}$ and every monomer in a *i*P2VP track was protonated; (b) *i*P2VP/(-)-CSA$_{80}$/Azo-SO$_3$H$_{20}$ and one monomer in five in a *i*P2VP track was protonated; (c) *i*P2VP/(-)-CSA$_{80}$/Azo-SO$_3$H$_{20}$, every monomer in a *i*P2VP track was protonated and the main chain of the track was restrained to keep the helical conformation. The polycation tracks and

the sulfonate ions were dissolved in 12500 chloroform molecules.

The simulations were performed by SPONGE[S5] and the general AMBER force field. [S6] The dihedral parameter of an azo group dihedral was set manually (force constant: 28 kcal·mol^{-1}, periodicity: 1 and phase: π) to mimic the *cis* photoisomerization. The atomic point charges were calculated by antechamber[S7] using AM1-BCC[S8,S9] charge model. The initial conformation was built by packmol. [S10] The smooth particle mesh Ewald (PME) [S11] method was used to evaluate the long-range Coulombic interactions. After 500000 steps minimization, the systems were equilibrated in the NPT ensemble for 1 ns with the time step of 1 fs, controlling the temperature to 300 K by the middle scheme of Langevin dynamics[13] and the pressure to 1 bar by the Berendsen barostat. [S12] For the production simulation, the first two cases (a) (b) were simulated for 250 ns and the last case (c) was simulated for 100 ns in the canonical ensemble.

The radial distribution function (RDF) between the S atoms of the Azo anions and the N atoms of the *i*P2VP tracks were calculated from the 250 ns trajectories. The RDF was defined as $g(r) = \frac{n_i(r)}{4\pi r^2 \delta r \rho}$, where $n_i(r)$ is the numbers of the target atoms between distances r and $r + \delta r$ and ρ is the bulk density for normalization.

The diffusion coefficient $D(\tau)$ was calculated from the Einstein's relation, $D(\tau) = MSD(\tau)/2E\tau$, where E is integer dimensionality of the diffusion and equals to 1 in the simulated systems. The coordinate of the sulfonate ions on the polymeric track was defined as the number of the nearest 2-vinylpyridine monomer. The distance between a sulfonate ion and a 2-vinylpyridine monomer was defined as the distance between the sulfur atom of the sulfonate ion and the nitrogen atom of the 2-vinylpyridine monomer.

4.2 Radial Distribution Function of the Azo sliders along the track

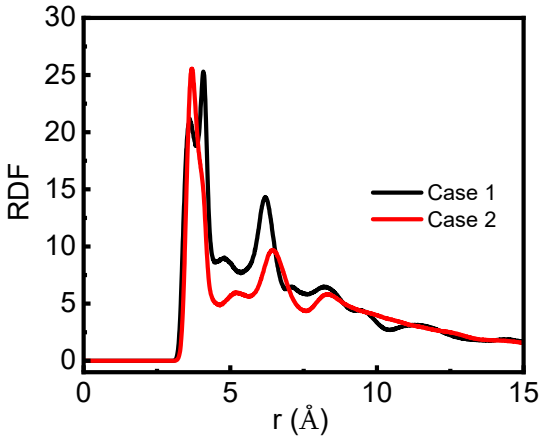

Figure S16 Radial Distribution Function between the S atoms of the Azo anions and the N atoms of the *i*P2VP tracks. **Case 1** and **Case 2** are shown in the blue and orange line respectively.

During the simulations, the Azo sliders are distributed near the iP2VP tracks both in **Case 1** and **Case 2**. The high peak and low minima indicate that tight ionic pairs are formed between Azo anions and the protonated pyridine monomers of the *i*P2VP tracks.

4.3 Diffusion of the Azo sliders along tracks in different protonated states

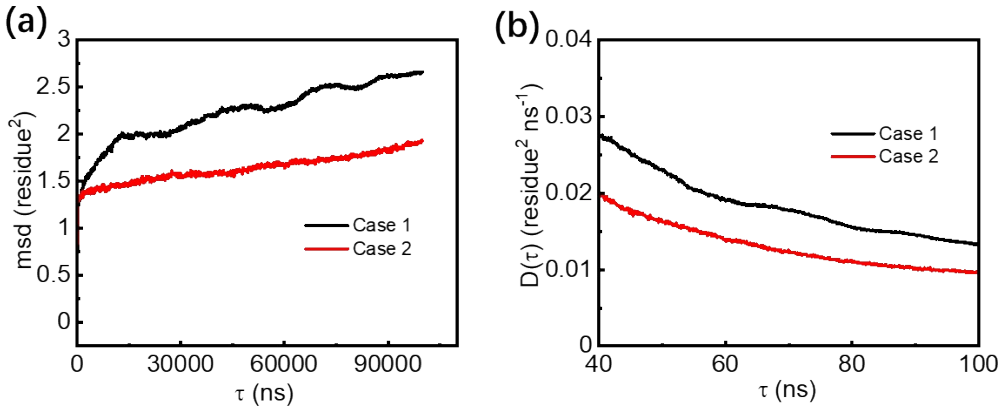

Figure S17 MD simulation of Azo sliders along tracks in different protonated states. (a, b) Mean squared displacement and diffusion coefficient $D(\tau)$ for 1D diffusion of Azo sliders along tracks. The Azo sliders along the tracks with CSA sliders, which every monomer was

protonated, showed higher mobility than those without CSA sliders, which every one in five monomer was protonated.

5. References

[S1] C. Yan, T. Q. Xu, X. B. Lu, *Macromolecules* **2018**, *51*, 2240–2246.

[S2] P. Li, Y. Song, S. Wang, Z. Tao, S. Yu, Y. Liu, *Ultrason. Sonochem.* **2015**, *22*, 132–138.

[S3] L. Hua, H. Ma, L. Zhang, *Chemosphere* **2013**, *90*, 143–149.

[S4] H. Kim, J. Gao, D. J. Burgess, *Int. J. Pharm.* **2009**, *377*, 105–111.

[S5] Y. P. Huang, Y. Xia, L. Yang, J. Wei, Y. I. Yang, Y. Q. Gao, *Chinese J. Chem.* **2022**, *40*, 160–168.

[S6] J. Wang, W. Wang, P. A. Kollman, D. A. Case, *J. Mol. Graph. Model.* **2006**, *25*, 247–260.

[S7] A. Jakalian, D. B. Jack, C. I. Bayly, *J. Comput. Chem.* **2002**, *23*, 1623–1641.

[S8] A. Allouche, *J. Comput. Chem.* **2012**, *32*, 174–182.

[S9] U. Essmann, L. Perera, and M. L. Berkowitz *J. Comput. Chem.* **2012**, *32*, 174–182.

[S10] Z. Zhang, X. Liu, Z. Chen, H. Zheng, K. Yan, and J. Liu, *J. Chem. Phys.* **2017**, *147,* 034109.

[S11] H. J. C. Berendsen, J. P. M. Postma, W. F. van Gunsteren, A. DiNola, and J. R. Haak , *J. Chem. Phys.* **1984,** *81*, 3684-3690.